Physica Scripta

PAPER

First principle study of half metallic ferromagnetism and transport properties of spinel's $ZnFe_2(S/Se)_4$ for spintronic

To cite this article: Abeer A AlObaid *et al* 2021 *Phys. Scr.* **96** 125816

Physica Scripta

PAPER

First principle study of half metallic ferromagnetism and transport properties of spinel's $ZnFe_2(S/Se)_4$ for spintronic

Abeer A AlObaid[1], **Tahani I Al-Muhimeed**[1], **Abdur Rahim**[2], **Ghazanfar Nazir**[3,4], **S Bouzgarrou**[5,6], **Abeer Mera**[7,8], **A I Aljameel**[9], **H H Hegazy**[10,11], **G Murtaza**[2,12] and **Qasim Mahmood**[13]

[1] Department of Chemistry, College of Science, King Saud University, PO Box 22452, Riyadh 11451, Saudi Arabia
[2] Materials Modeling Lab, Department of Physics, Islamia College Peshawar 25120, Khyber Pakhtunkhwa, Pakistan
[3] Department of Chemistry, Inha University, 100 Inharo, Incheon, 22212, Republic of Korea
[4] Department of Physics, Korea Advanced Institute of Science and Technology (KAIST), Daejeon 34141, Republic of Korea
[5] Laboratoire de Microélectronique et Instrumentation (UR 03/13-04), Faculté des Sciences de Monastir, Avenue de l'Environnement 5000 Monastir, Tunisia.
[6] Department of Physics, College of Science, Qassim University, P. O. 64, Buraidah, Saudi Arabia
[7] Department of Physics, College of Arts and Science, Prince Sattam Bin Abdulaziz University, Wadi Addawasir, 11991, Kingdom of Saudi Arabia, Saudi Arabia
[8] Department of Physics, Faculty of Science, Kafrelsheikh University, Kafrelsheikh 33516; Egypt
[9] Department of Physics, College of Science, Imam Mohammad Ibn Saud Islamic University (IMSIU), Riyadh 11623, Saudi Arabia
[10] Department of Physics, Faculty of Science, King Khalid University, PO Box 9004, Abha, Saudi Arabia
[11] Department of Physics, Faculty of Science, Al-Azhar University; 71524, Assiut; Egypt
[12] Department of Mathematics & Natural sciences, Prince Mohammad Bin Fahd University, P. O. Box 1664, Alkhobar 31952, Saudi Arabia
[13] Basic & Applied Scientific Research Center, and Department of Physics, Imam Abdulrahman Bin Faisal University, PO Box 1982, 31441 Dammam, Saudi Arabia

E-mail: zafarforall2004@gmail.com

Keywords: spinels, DFT, Half metallicity, spintronics, thermoelectric efficiency

RECEIVED
11 July 2021

REVISED
11 August 2021

ACCEPTED FOR PUBLICATION
7 September 2021

PUBLISHED
16 September 2021

Abstract

Half metallic ferromagnetism received remarkable attention due to its immense technological applications in spintronic. In this perspective, thiospinels $ZnFe_2S/Se_4$ is addressed by employing density functional theory (DFT) for spintronics and thermoelectric devices. The optimized energy versus volume leads to the confirmation of the Ferromagnetic (FM) states stability of both spinels. The formation energy confirms the thermodynamic stability. TDOS and PDOS are determined to confirm spin polarization and half-metallic ferromagnetism. Ferromagnetism is explored by exchange energies and magnetic moments. In addition, thermoelectric characteristics are explored by electrical and thermal conductivities, Seebeck coefficient, and power factor to evaluate their potential in thermo-electric applications.

1. Introduction

Spintronic is an emerging field in the scientific research community and is defined as a novel type of electronics that manipulates electrons by charge and spin of the electrons [1–3]. Its recent development begins since in 1988 with the invention of GMR. [4]. Half metal can be defined in terms of spin polarization (SP). Spin-polarized leads to resolving the heat problems that occur in IC and various electronic devices. Materials with high spin polarization, high magnetic phase transition (close to room temperature), and high magnetic moment are required to utilize in spintronic technology. Materials which do not exhibit spin polarization are diamagnetic because of unchanged DOS in both channels. However, asymmetric exist in ferromagnetic materials because of the exchange mechanism which limits SP less than unity. On the other hand, half-metallic contains states at the Fermi level in one channel and insulators in the second channel [5]. Thus, the materials persist 100% polarization and are highly recommended materials for spintronics. The discovery of half metals made a great contribution to the field of spintronics due to their technological implications in efficient spintronic devices including magnetic recording, electronic memory, and effective magnetic sensor [6–8].

Over the last few decades, researchers have been focused on many compounds, including (half, full and quaternary) Heusler alloys [9, 10], dilute semiconductor [11], transition metal oxides [12], Spinels FeO_4 [13], perovskites $BaBkO_3$ [14], double perovskites [15] and halide double perovskites [16]. Looking for half metal's materials with high Curie temperature at RT has been focused on for more than 15 years. A special class of materials called spinels with cubic structures generalized by the formula AB_2O_4 with unique properties has attracted more attention [17, 18]. To tune the physical properties of such complex crystals their present multiple degrees of freedom. This class of materials has diverse properties including its potential application in photocatalytic degradation [19–21], charge storing devices [22], thermoelectricity [23] energy conversion applications [24]. Thiospinels have several desirable optical properties, including transparency across at large photosensitivity [25], and nonlinear optical susceptibility [26] all of which make them capable candidates for optoelectronic devices. Thiospinels (Zn/Hg) In_2S_4 are used in terms of transport properties for energy conversion devices [27]. Moreover, XIn_2S_4(X = Cd, Mg) has the potential ability for optoelectronic devices [28].

Ferromagnetism materials with semiconducting nature are the best option for spintronic applications. The ferromagnetic spinel semiconductors AB_2X_4 (A = Cu, Hg, Cd, B = Cr, and X = S, Se) are well-known magnetic semiconductors, for instance, $CuCr_2Se_4$ [29–31]. Further, the Curie temperature range 84 K–430 K, and ferromagnetic semiconductor behavior make them appealing for spintronics [32]. Spinel ferromagnetic materials play a key role regarding ferroelectric, memory, and spintronic applications [33, 34]. Owing to Colossal Magnetoresistance in the transition metal ferro-spinel materials offers a fascinating platform for researchers [35, 36]. The ferromagnetic characteristics of $MgCr_2S_4$ and $MgMn_2S_4$ are considered excellent FM [37, 38]. Q. Mahmood *et al* worked on ferromagnetism in $MgCr_2X_4$(X = S, Se) [39]. Recently, Mehmood *et al* demonstrated the magnetic behavior of $MgPr_2(S/Se)_2$ for spintronic applications by DFT calculation [40]. Moreover, various properties of Spinels $Ca(V/Mn)_2S_4$ have been investigated computationally including structural, magnetic, and thermoelectric [41].

The above vibrant review ensures that there is no literature available on Spinel's $ZnFe_2S/Se_4$ regarding their half-metallic ferromagnetism and transport properties. In this article, we used TB-mBJ to determine electronic band structures, the partial and total density of states, and the half-metallic character of Zn-based thiospinels. The ferromagnetism due to exchange mechanism and spin polarization without clustering effect is the primary goal of our research. Thermoelectric parameters are investigated by employing BoltzTrap code. The study of the effect of temperature, and thermal conductivity on the spin of electrons large effect the reliability of the devices. Therefore, the effects of these parameters are also discussed in detail. The theoretical data presented in this work can cover the lack of physical properties information on the $ZnFe_2S/Se_4$ compounds.

2. Computational details

We employed the full-potential linearized augmented plane wave method FP-APW realized in the WIEN2K package within the framework of DFT to calculate various properties including structural, electronic, magnetic, and thermoelectric [42–44]. For reducing interatomic forces in electronic structures, optimization has been done through PBEsol approximation. The structural characteristics are calculated by Perdew–Burke–Ernzerhof PBEsol [45, 46] and modified Becke Johnson potential of Trans and Blaha (TB-mBJ) [47] because PBEsol was analyzed the ground state properties more accurately but underestimate the electronic bandgap. Therefore, to improve the bandgap accurately, the TB-mBJ potential has been implemented over the PBEsol approximation. The solution of the electronic system inside the muffin-tin region is taken spherically harmonic. The k-mesh of the order $12 \times 12 \times 12$ has been selected as the point at which the energy is released by the system [48]. The convergence parameters are adjusted as $K_{max}xR_{MT} = 8.0$, muffin radius (R_{MT}), and K_{max} wave vector in the reciprocal lattice, Gaussian factor $G_{max} = 18$, and angular momentum $\ell_{max} = 10$. The change was converged up to 0.001m Ry. Furthermore, the TB-mBJ converged energy and the optimized electronic structures were used to calculate the thermoelectric behavior through classical Boltzmann transport theory by using BoltzTraP Package [49].

3. Result and discussion

3.1. Structural analysis

To optimize the cubic crystal structure of thiospinels $ZnFe_2(S/Se)_4$ with Fd-3m space group we have used PBEsol approximation. The crystal structure of the Zn-based thiospinels is presented in figure 1. The relaxation process is used for atomic positions with Zn (0.125, 0.125, and 0.125), Fe (0.5, 0.5, and 0.5) and O (0.25, 0.25, and 0.25) which are in accordance with the space group Fd-3m.

The optimized $ZnFe_2(S/Se)_4$ for FM and AFM states are presented in figure 2. The planned analogy of FM and AFM revealed that $ZnF_2(S/Se)_4$ possess ferromagnetic nature owing to their lower energy. Similar results are

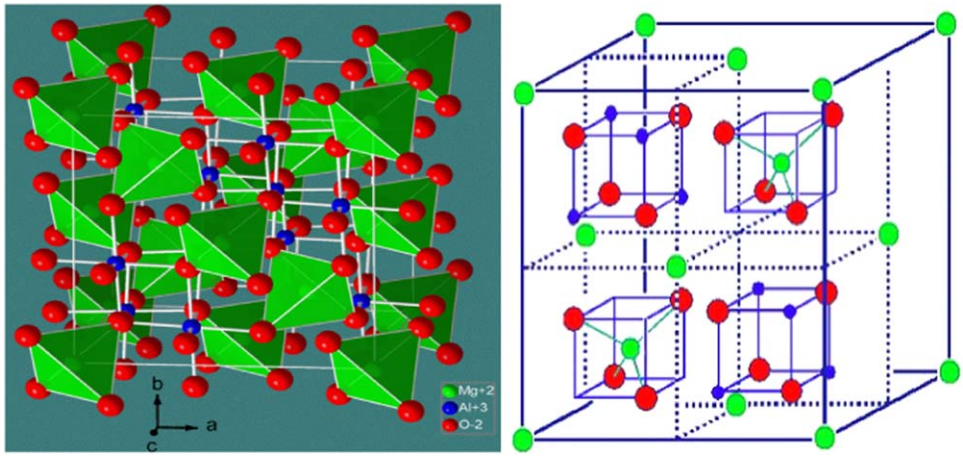

Figure 1. the crystal structure in atomic form and polyhedral form of cubic Spinels $ZnFe_2S/Se_4$.

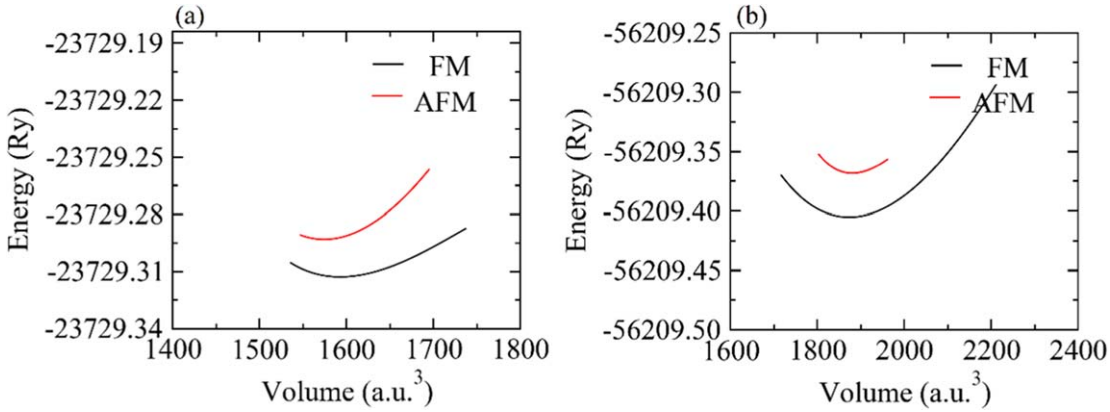

Figure 2 . Optimized plots in FM (black color) and AFM (red color)states of (a) $ZnFe_2S_4$ and (b) $ZnFe_2Se_4$.

evident from the literature of XCr_2O_4 (X = Zn, Cd), and AV_2O_4 (A = Zn, Cd, Hg) which ensure the lowest energy in FM states confirm its stability. Therefore, the consistency of calculated results with the existing literature is proof of the reliability of the study [50, 51].

The formation energy of studied compounds have been calculated by the relation

$$\Delta H_f = E_{Total}(Zn_lFe_mS/Se_n) - lE_{Zn} - mE_{Fe} - nE_{S/Se} \quad (1)$$

Where $E_{Total}(Zn_lFe_mS/Se_n)$, E_{Zn}, E_{Fe} and $E_{S/Se}$ are the energies of $ZnFe_2S/Se_4$, Zn, Fe, and S/Se, respectively. The computed values are −3.4 eV for $ZnFe_2S_4$, and −3.1 eV for $ZnFe_2Se_4$ which confirm that studied materials are thermodynamically favorable [52]. Furthermore, we have computed the Curie temperature by the Classical Heisenberg model whose mathematical form is $Tc = \Delta E/3K_B$, where ΔE is the energy difference between paramagnetic and ferromagnetic states, K_B is Boltzmann constant [53]. The computed values are 315 K, and 305 K which show the room temperature ferromagnetism.

3.2. Electronic bandstructure

Band structure analysis is an important step in the understanding of material nature and its suitability for device applications. Due to the ferromagnetic nature of these materials, we have calculated spin-up and spin-down band structures presented in figures 3(a), (b). The valence band maxima (VBM) lie at the K-symmetry point while conduction band minima (CBM) at Gamma point in the up-spin channel of $ZnFe_2S_4$ shown in figure 3(a). In addition, the VBM lies between Gamma-X points while CBM lies at Gamma points in down-spin channels showing a semiconductor nature. Similarly, the up spin and down spin channels are plotted for $ZnFe_2Se_4$ schemed in figure 3(b). In the up-spin channel, the VBM stays on the K-symmetry point crossing the Fermi level and CBM stays on Gamma-symmetry. Whereas, in the down spin channel both the VBM and CBM lie at Gamma symmetry point having a narrow gap about Fermi level leading to semiconducting nature. Therefore, by

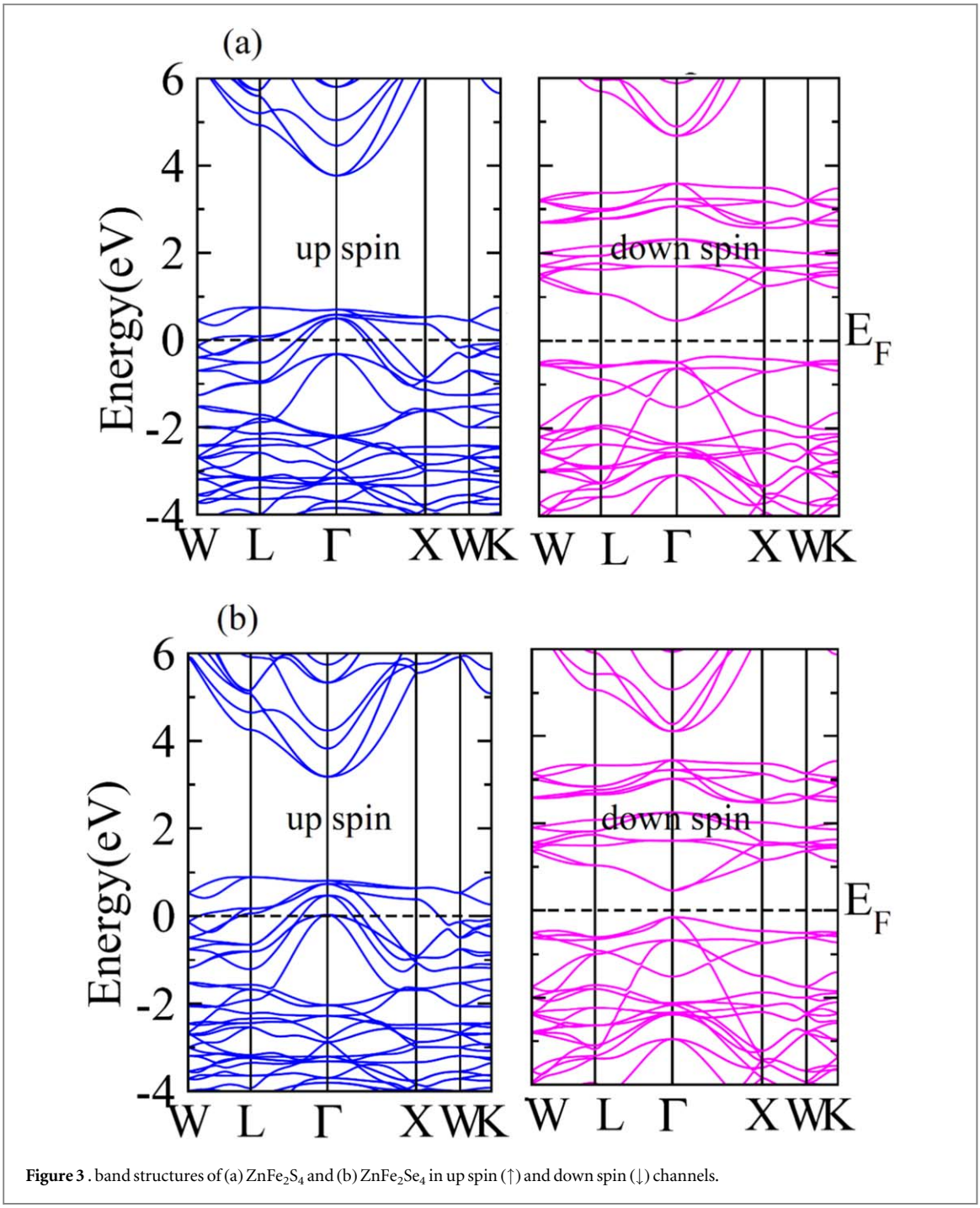

Figure 3 . band structures of (a) $ZnFe_2S_4$ and (b) $ZnFe_2Se_4$ in up spin (↑) and down spin (↓) channels.

combining both insulating and semiconducting behavior of up spin and down spin channels form ferromagnetic materials.

Materials with maximum spin polarizability are desirable for spintronic applications. The spin polarizability be calculated by the given mathematical relation [54],

$$P = \frac{N(\uparrow)E_F - N(\downarrow)E_F}{N(\uparrow)E_F + N(\downarrow)E_F} \times 100\% \quad (2)$$

Where $N(\uparrow)$ and $N(\downarrow)$ stand for the total density of states (TDOS). To take a clearer picture of half-metallicity and exchange mechanism in these thiospinels, we have plotted the total and partial density of states (PDOS) in figures 4(a)–(b). The Fermi level is present in the valence band for the up spin channel, and in the forbidden region for the down spin channel. The value of P is 100% for both compounds make them promise for spintronics. The distribution of valence and conduction states reveals that TDOS indicates half-metallic behavior in these spinels-like band structures.

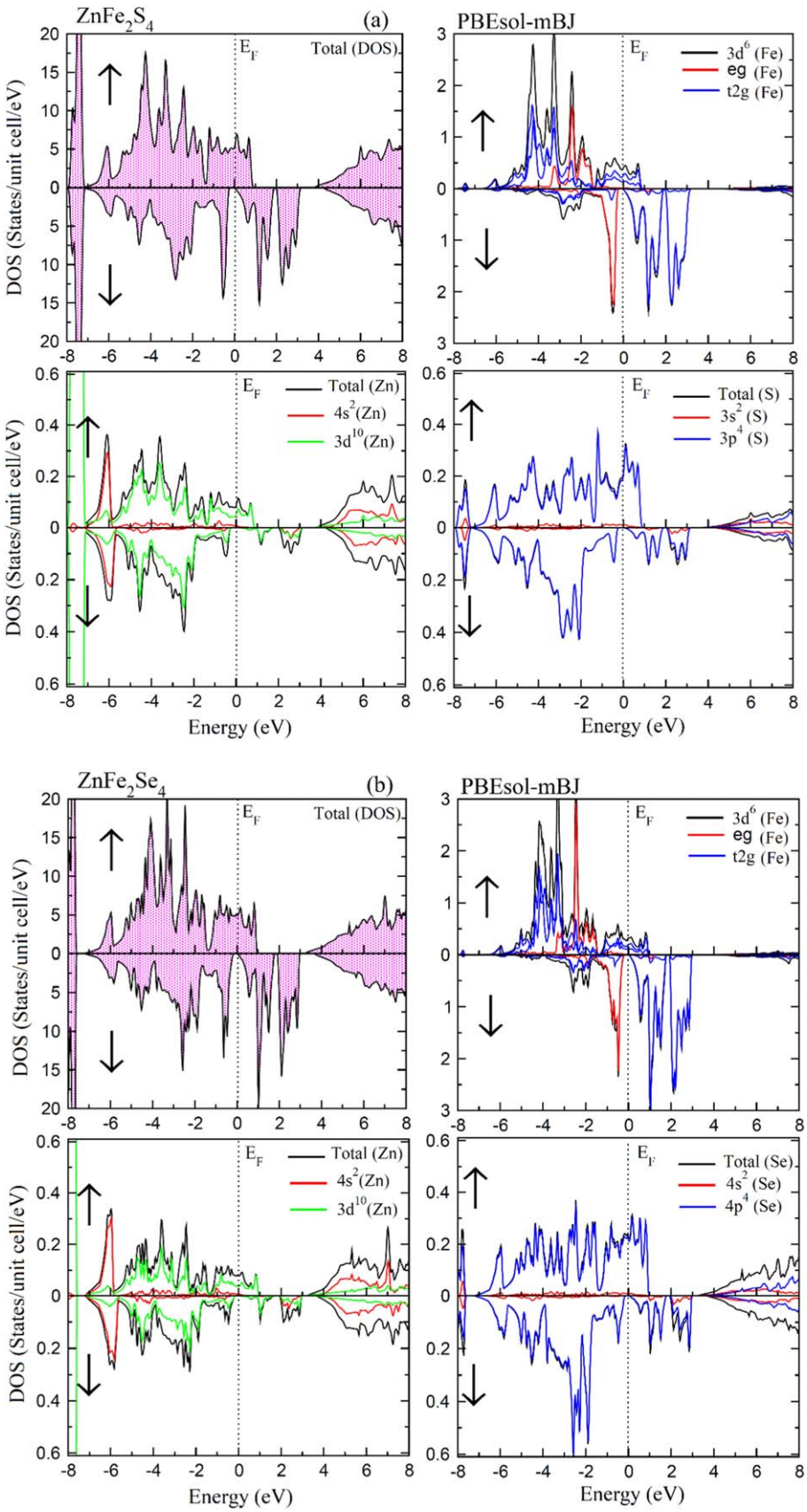

Figure 4. (a) DOS of $ZnFe_2S_4$ in up spin (↑) and down spin (↓) channel. (b) DOS of $ZnFe_2Se_4$ in up spin (↑) and down spin (↓) channels.

3.3. Magnetic properties

Magnetic properties of materials are crucial for determining their suitability to spintronic applications. To explain magnetism in materials two potential exchanges, play a vital role, e.g double-exchange and super

Table 1. The computed values of exchange energies ($\Delta E_{crystal}$, $\Delta_x(d)$, $\Delta_x(pd)$, and exchange constants ($N_o\alpha$ and $N_o\beta$) for $ZnFe_2S/Se_4$.

Compounds	($\Delta E_{crystal}$)	$\Delta_x(d)$	$\Delta_x(pd)$	$N_o\alpha$	$N_o\beta$
$ZnFe_2S_4$	−1.80	3.65	−0.027	−0.97	−0.34
$ZnFe_2Se_4$	−2.13	3.51	−0.046	−0.95	−0.37

exchange [55]. Super-exchange is responsible for anti-ferromagnetism while the double exchange generates ferromagnetism [56–58]. The FM nature of present thiospinels is confirmed through an optimization process. This FM nature arises due to the double exchange mechanism in these materials, where transition metal's d orbital split into degenerate triplet t_{2g} (d_{xy}, d_{yz}, d_{xz}) states and doublet states $e_{.g.}$ (d_z^2 and d_x^2–d_y^2). The $3d^6$ states of Fe atom contribute sharp peaks in the up and down spin channel ranges from (1 to −6) eV showing metallic behavior in up spin channel.

The splitting of $e_{.g.}$ (Fe) and t_{2g} (Fe) in the down spin channel cause a narrow bandgap which shows the presence of semiconducting nature in spin-down configuration. The occurrence of $e_{.g.}$(Fe) and 3d(Fe) states at separate energies ensures the magnetic moment of electrons exist which causes ferromagnetic character. From PDOS the $3d^6$, $e_{.g.}$, t_{2g} states of Fe are majorly responsible FM nature. In the individual PDOS of Zn, the valence band of total (Zn) states possesses high peaks crossing Fermi level, which confirm metallic nature in the up-spin configuration, while in the downward configuration it shows semiconducting behavior. However, the contribution of $4s^2$ (Zn) is minimum in both configurations. The total and partial contribution of the S atom is displayed in figure 4, where $3p^4$ state majorly presents high peaks in both channels.

By replacing S with Se, a similar pattern of results is obtained for $ZnFe_2Se_4$ through the density of states. The TDOS holds metallic nature in the majority spin region while a semiconducting nature in the minority spin region due to hybridization among Fe, Zn, and Se. It is important to highlight the PDOS of $ZnFe_2Se_4$, which are sketched for Fe, Zn, and Se individually in figure 4(b). The first is one is for Fe where the $3d^6$ state possesses high peaks in the low range of energy states (lower than −1) and crossing the Fermi level with lower intensity in the up-spin channel. It can be seen from figure 4 that narrow gap raised due to hybridization of doublet state of $e_{.g.}$(Fe) and triplet state of t_{2g}(Fe) in bonding and in an anti-bonding state in spin-down configuration near the E_F, respectively. Further, Zn total and $3d^{10}$ (Zn) major peaks fluctuated in the lower energy range in up and down spin configuration. These peaks shifting beyond Fermi level with lower energy causes metallic nature in up spin configuration. The contribution due to $4s^2$(Zn) is lower near the Fermi level. Finally, the individual PDOS of Se demonstrates the Total (Se), $4s^2$(Se), and $4p^4$(Se) states. Total (Se) plays an important role in anti-bonding states in high energy states, while the $4s^2$(Se) state indicates a small contribution. The $4p^4$(Se) state is responsible for major peaks in both channels with metallic in up spin channel and semiconducting in a downward channel. Overall, this half-metallic character is due to the separating of d states orbitals of Fe and Zn in the existence of the external force of four Se atoms. As Fe-d states split into $e_{.g.}$ (d_z^2 and d_{x-dy}^2) states t_{2g} (d_{xy}, d_{yz}, and d_{xz}) states [58]. Thus, crystal field energy ΔCF arises from the splitting of e.g. states and t_{2g} states and can be defined in terms of the difference between the two states i.e., ($\Delta E = e_g - t_{2g}$) [59].

The behavior of ferromagnetism provokes by this crystal field energy and can be decreased by $\Delta_x(d)$ is presented in table 1. The condition was evident for introducing ferromagnetism [60].

It is important to highlight the term exchange energy $\Delta_x(pd)$ among the d states of Fe/Zn and 4p state of Se. The negative value confirms the occurrence of ferromagnetism. From table 1, it can be seen that ΔCF decreases from $ZnFe_2S_4$ to $ZnFe_2Se_4$, which indicates that Se-based spinels are more favorable for ferromagnetism. The exchange constants $N_0\alpha$ and $N_0\beta$ are calculated by [61].

$$N_0\alpha = \frac{\Delta E^c}{xS},\ N_0\beta = \frac{\Delta E^v}{xS} \tag{3}$$

Where x and S stand for the concentration and magnetic moment of Fe atom. While $\Delta E^c = E_\downarrow^c - E_\uparrow^c$ and $\Delta E^v = E_\downarrow^v - E_\uparrow^v$ are the energies at VB and CB edges. In table 1. One can see the calculated values of $N_0\alpha$ and $N_0\beta$. According to Zenger's exchange model (extensively used theory of the ferromagnetism in ferromagnetic semiconductors) [62, 63] the negative value of $N_0\beta$ show the magnetic impurity through the energy gap in the down spin channel with lower energy. The total magnetic moment of these compounds was calculated to analyze ferromagnetic strength which arises due to MM of individual atoms and interstitial regions. From table 2. It is obvious that Fe is the most contributor to the TMM in both spinels while minor contribution comes from the Zn and interstitial regions.

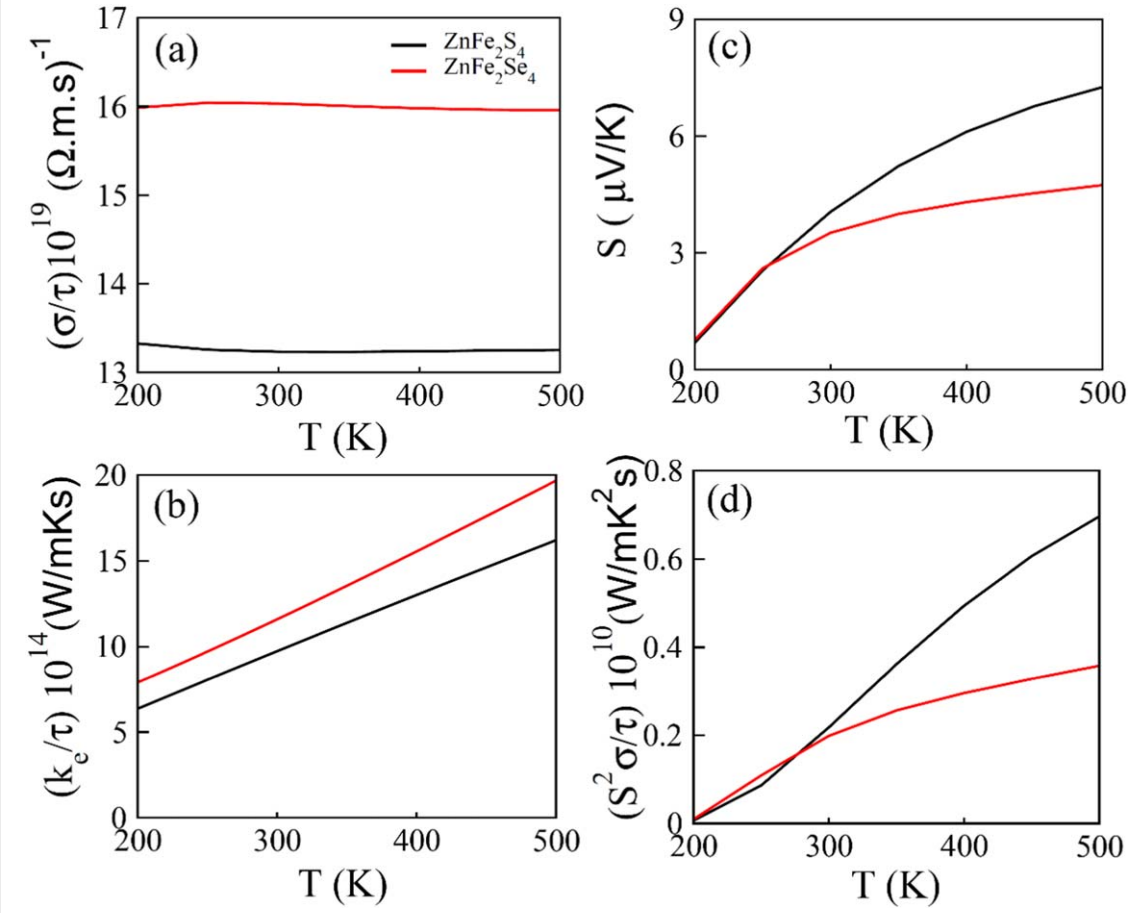

Figure 5. The computed (a) σ/τ, (b) κ/τ, (c) S, and (d) $\sigma S^2/\tau$ of $ZnFe_2S/Se_4$.

Table 2. The magnetic moments for, Zn, Fe, S/Se. $ZnFe_2S_4$ and $ZnFe_2Se_4$.

	Total (μ_B)	Int (μ_B)	Cs (μ_B)	Fe (μ_B)	(S/Seμ_B)
$ZnFe_2S_4$	4.00	0.057	0.001	3.03	0.023
$ZnFe_2Se_4$	4.00	0.331	0.003	2.80	0.027

3.4. Thermoelectric properties

To overcome the global energy crises, the transformation of heat energy into useful electrical energy is an effective way. Therefore, we investigated the thermoelectric behavior of spinels $ZnFe_2(S/Se)_4$ through BoltzTrap code [49]. The thermoelectric parameters are plotted against temperature shown in figures 5(a)–(d). The plotted electrical conductivity against temperature demonstrates a small variation in the range of 200 K to 300 K and remains steady for high temperature in the case of both spinels. The thermal conductivity (k) of materials is the heat flow (q) due to the temperature gradient following the Fourier law $q = -k\nabla_x(T)$.

Here, the computed thermal conductivity value increases linearly with the temperature range presented in figure 5(b) for both $ZnFe_2S_4$ and $ZnFe_2Se_4$ from $6.5 \times 10^{14}(W/mKs)$ to $16 \times 10^{14}(W/mKs)$ and $7.5 \times 10^{14}(W/mKs)$ to $20 \times 10^{14}(W/mKs)$, respectively. Further, the Seebeck coefficient S explains voltage due to temperature gradient and can be calculated via the given equation.

$$S = \left(\frac{8}{3eh^2}\right)\pi^2 K_B^2 m^* T\left(\frac{\pi}{3n}\right)^{\frac{1}{2}} \tag{4}$$

Where e, h, K_B, m^*, T, and n are electronic charge, Planck constant, Boltzmann constant, effective mass, absolute temperature, and carrier concentration, respectively. Seebeck coefficient of $ZnFe_2(S/Se)_4$ are plotted in figure 5(c). The computed value of S has the same value for both spinels up to 260 K. Next, the values of $ZnFe_2S_4$ and $ZnFe_2Se_4$ differed and reached at $7.2(\mu\ V/K)$ and $4.5(\mu\ V/K)$ at 500 K, respectively. Furthermore, the Power factor plays a key role in an understanding of thermoelectric performance with a mathematical expression of $P = S^2\sigma/\tau$. The calculated value of P for $ZnFe_2S_4$ started from 0 W/mK^2s at 200 K and obtained a

maximum value of $0.7 W/mK^2 s$ at 500 K. For $ZnFe_2Se_4$ the estimated values of P lies in range of $(0 - 0.35) W/mK^2 s$ in the whole temperature range. Hence, the figure of merit ZT is directly proportional to the power factor. Thus, materials with high power factors are suitable for energy conversion devices. In our case, $ZnFe_2S_4$ is a potential candidate for such an application.

4. Conclusion

In this research article, we have investigated structural, electronic, magnetic, and thermoelectric properties of $ZnFe_2(S/Se)_4$ for spintronic and thermoelectric applications. The optimization of energy versus volume plots reveals that these spinels are favorable for ferromagnetism. The electronic band structures were calculated in terms of spin-up and down orientation with a narrow bandgap. The half-metallicity was confirmed by TDOS and PDOS with one channel having 100% spin polarization. The magnetic moment on nonmagnetic and interstitial sites has been reported. The electrical conductivity has not shown much variation with temperature. However, thermal conductivity, Seebeck coefficient, and the power factor increased with increasing temperature leading to high thermoelectric performance.

Acknowledgments

The authors extend their appreciation to the Researchers Supporting Project number (RSP-2021/381), King Saud University, Riyadh, Saudi Arabia. The author (H. H. Hegazy) extends his appreciation to the Deanship of Scientific Research at King Khalid University for the financial support through research groups program under grant number (G.R.P/199/42).

Data availability statement

The data that support the findings of this study are available upon reasonable request from the authors.

ORCID iDs

G Murtaza https://orcid.org/0000-0001-5520-2265
Qasim Mahmood https://orcid.org/0000-0001-7449-5876

References

[1] Das S S 2001 Spintronics: a new class of device based on electron spin, rather than on charge, may yield the next generation of microelectronics *Am. Sci.* **89** 516–23
[2] Joshi K V 2016 Spintronics: a contemporary review of emerging electronics devices *Engineering Science and Technology, an International Journal* **19** 1503–13
[3] Wolf S A, Awschalom D D, Buhrman R A, Daughton J M, Molnár V, Roukes M L, Chtchelkanova A Y and Treger D M 2001 Spintronics: a spin-based electronics vision for the future *Science* **294** 1488–95
[4] Roqan I S, Venkatesh S, Zhang Z, Hussain S, Bantounas I and Franklin J B 2015 Obtaining strong ferromagnetism in diluted Gd-doped ZnO thin films through controlled Gd-defect complexes *J. Appl. Phys.* **117** 073904
[5] De Groot R A, Mueller F M, Van Engen P G and Buschow K H J 1983 New class of materials: half-metallic ferromagnets *Phys. Rev. Lett.* **50** 2024
[6] Venkatesh S, Franklin J B, Ryan M P, Lee J S, Ohldag H and McLachlan M A 2015 Defect-band mediated ferromagnetism in Gd-doped ZnO thin films *J. Appl. Phys.* **117** 013913
[7] Kobayashi K I, Kimura T, Sawada H, Terakura K and Tokura Y 1998 Room-temperature magnetoresistance in an oxide material with an ordered double-perovskite structure *Nature* **395** 677–80
[8] Pickett W E and Moodera J S 2001 Half metallic magnets *Phys. Today* **54** 39–45
[9] Saleem Y and Gupta D C 2018 Insight into half-metallicity, spin-polarization, and mechanical properties of L21 structured MnY_2Z (Z = Al, Si, Ga, Ge, Sn, Sb) Heusler alloys *J. Alloys and Compounds* **735** 1245–52
[10] Quyoom S A and Gupta D C 2019 Exploration of highly correlated Co-based quaternary Heusler alloys for spintronics and thermoelectric applications *Int. J. Energy Res.* **43** 8864–77
[11] Lin-Hui Y, Freeman A J and Delley B 2006 Half-metallic ferromagnetism in Cu-doped ZnO: density functional calculations *Phys. Rev. B* **73** 033203
[12] Ji Y, Strijkers G J, Yang F Y, Chien C L, Byers J M, Anguelouch A, Xiao G and Gupta A 2001 Determination of the spin polarization of half-metallic CrO_2 by point contact Andreev reflection *Phys. Rev. Lett.* **86** 5585
[13] Mahmood Q, Haq B U, Rashid M, Noor N A, AlFaify S and Laref A 2020 First-principles study of magnetic and thermoelectric properties of $SnFe_2O_4$ and $SnCo_2O_4$ spinels *Journal of Solid-State Chemistry* **286** 121279
[14] Muskan N, Bhat T M and Gupta D C 2019 Magneto-electronic, thermodynamic, and thermoelectric properties of 5 f-electron system $BaBkO_3$ *J. Supercond. Novel Magn.* **32** 1751–9
[15] Abbas S, Motlagh S Y and Badfar H 2019 Ferro hydro dynamic analysis of heat transfer and biomagnetic fluid flow in channel under the effect of two inclined permanent magnets *J. Magn. Magn. Mater.* **472** 472115–22

[16] Ahmad M S and Gupta D C 2021 Analysis of cage structured halide double perovskites Cs_2NaMCl_6 (M = Ti, V) by spin polarized calculations J *Alloys and Compounds* **854** 156000
[17] Hosseini S M 2008 Structural, electronic, and optical properties of spinel $MgAl_2O_4$ oxide *Physica status solidi (b)* **245** 2800–7
[18] Wang Y, Chen W B, Liu F Y, Yang D W, Tian Y, Ma C G, Dramicanin M D and Brik M G 2019 High-throughput first-principles calculations as a powerful guiding tool for materials engineering: Case study of the AB_2X_4 (A = Be, Mg, Ca, Sr, ba; B = Al, Ga, in; X = O, S) spinel compounds *Results in Physics* **13** 102180
[19] Fang F, Chen L, Chen Y B and Wu L M 2010 Synthesis and photocatalysis of $ZnIn_2S_4$ nano/micro peony *J. Phys. Chem. C* **114** 2393–7
[20] Wen-Juan F, Zhou Z F, Xu W B, Shi Z F, Ren F M, Ma H H and Huang S W 2010 Preparation of $ZnIn_2S_4$/fluoropolymer fiber composites and its photocatalytic H_2 evolution from splitting of water using Xe lamp irradiation *Int. J. Hydrogen Energy* **35** 6525–30
[21] Zhibin L, You W, Liu M, Zhou G, Takata T, Hara M, Domen K and Li C 2003 Photocatalytic water reduction under visible light on a novel $ZnIn_2S_4$ catalyst synthesized by hydrothermal method *Chem. Commun.* **17** 2142–3
[22] Zhang Z, Schwingenschlögl U and Roqan I S 2014 Vacancy complexes induce long-range ferromagnetism in GaN *J. Appl. Phys.* **116** 183905
[23] Aravindh A S D, Schwingenschloegl U and Roqan I S 2015 Defect induced d0 ferromagnetism in a ZnO grain boundary *J. Chem. Phys.* **143** 224703
[24] Masood Y, Saeed M A, Isa A R M, Aliabad H A R and Sahar M R 2013 An insight into the structural, electronic and transport characteristics of XIn_2S_4 (X = Zn, Hg) thiospinels using a highly accurate all-electron FP-LAPW + Lo method *Chin. Phys. Lett.* **30** 077402
[25] Seok-Joo L, Kim J E and Park H Y 2003 Optical absorption of Co^{2+} in $MgIn_2S_4$, $CdIn_2S_4$, and $HgIn_2S_4$ spinel crystals *J. Mat. Research* **18** 733–6
[26] Mahmood Q, Umm-eHani, Al-Muhimeed Tahani A I, AlObaid A, Haq B U, Murtaza G, Flemban T H and Althib H 2021 Study of optical and thermoelectric properties of $ZYbI_3$ (Z = Rb, Cs) for solar cells and renewable energy; Modelling by density functional theory *J. Phys. Chem. Solids* **155** 110117
[27] Mahmood Q, Hassan M, Algrafy E, Haq B U, Kattan N A, Murtaza G and Laref A 2020 Theoretical investigations of optoelectronic and thermoelectric properties of the XIn_2O_4 (X = Mg, Zn, Cd) spinel oxides *J. Phys. Chem. Solids* **144** 109481
[28] Masood Y, Dalhatu S A, Murtaza G, Khenata R, Sajjad M, Musa A, Aliabad H A R and Saeed M A 2015 Optoelectronic properties of XIn_2S_4 (X = Cd, Mg) thiospinels through highly accurate all-electron FP-LAPW method coupled with modified approximations. *J. Alloys Compd.* **625** 182–7
[29] Samokhvalov V, Dietrich M, Schneider F and Unterricker S 2005 The ferromagnetic semiconductor $HgCr_2Se_4$ as investigated with different nuclear probes by the PAC method *Hyperfine Interact.* **160** 17–26
[30] Park Y D, Hanbicki A T, Mattson J E and Jonker B T 2002 Epitaxial growth of an n-type ferromagnetic semiconductor $CdCr_2Se_4$ on GaAs (001) and GaP (001) *Appl. Phys. Lett.* **81** 1471–3
[31] Samokhvalov V, Unterricker S, Burlakov I, Schneider F, Dietrich M, Tsurkan V and Tiginyanu I M 2003 And ISOLDE collaboration investigation of ferromagnetic spinel semiconductors by hyperfine interactions of implanted nuclear probes *J. Phys. Chem. Solids* **64** 2069–73
[32] Ali S, Rashid M, Hassan M, Noor N A, Mahmood Q, Laref A and Haq B U 2018 Ab-initio study of electronic, magnetic, and thermoelectric behaviors of LiV_2O_4 and $LiCr_2O_4$ using modified Becke-Johson (mBJ) potential *Physica B* **537** 329–35
[33] Peter L, Fichtl L, Hemberger J, Tsurkan V and Loidl A 2005 Relaxation dynamics and colossal magnetocapacitive effect in $CdCr_2S_4$ *Phys. Rev. B* **72** 060103
[34] Sun C P, Huang C L, Lin c.c., Her J L, Ho C J, Lin J Y, Berger H and Yang H D 2010 Colossal electroresistance and colossal magnetoresistance in spinel multiferroic $CdCr_2S_4$ *Appl. Phys. Lett.* **96** 122109
[35] Hossain A, Seki M, Kawai T and Tabata H 2004 Colossal magnetoresistance in spinel type $Zn_{1-x}Ni_xFe_2O_4$ *J. Appl. Phys.* **96** 1273–5
[36] Helmolt V, Wecker R J, Holzapfel B, Schultz L and Samwer K 1993 Giant negative magnetoresistance in perovskitelike $La_{2/3}Ba_{1/3}MnO_x$ ferromagnetic films *Phys. Rev. Lett.* **71** 2331
[37] Mahmood Q, Murtaza G, Ali G, Hassan M, Algrafy E, Shahid M S, Kattan N A K and Laref A 2020 Probing the electronic structure and magnetism in Ni doped ZnTe: A DFT modelling and experiment *J. Alloys and Compounds* **834** 155176
[38] Allison W, Key B, Phillips P J, Sa N, Lipton A S, Klie R F, Vaughey J T and Poeppelmeier K R 2018 Synthesis and characterization of $MgCr_2S_4$ thiospinel as a potential magnesium cathode *Inorg. Chem.* **57** 8634–8
[39] Mahmood Q, Noor N A, Jadan M, Addasi J S, Mahmood A and Ramay S M 2020 First-principle investigation of ferromagnetism and thermoelectric characteristics of $MgCr_2X_4$ (X = S, Se) spinels *J. Solid State Chem.* **285** 121261
[40] Mahmood A, Rashid M, Safder K, Waqas I M, Noor N A, Ramay S M, Masry W A and Al-Garadi N Y A 2021 Spin-dependent rare-earth-based $MgPr_2X_4$ (X = S, Se) spinels investigations for spintronic and sustainable energy systems applications *Results in Physics* **20** 103709
[41] Mahmood A, Ramay S M, Al-Masry W, Al-Zahrani A A and Al-Garadi N Y A 2020 Ab-initio computations of CaV_2S_4 and $CaMn_2S_4$ spinels for spintronics and energy storage system applications *J. Mater. Res. Techn* **9** 14783–91
[42] Peter B, Schwarz K, Madsen G K H, Kvasnicka D and Luitz J W2k 2001 An augmented plane wave + local orbitals program for calculating crystal properties **2001**
[43] Karlheinz S, Blaha P and Madsen G K H 2002 Electronic structure calculations of solids using the WIEN2k package for material sciences *Comput. Phys. Commun.* **147** 71–6
[44] Pierre H and Kohn W 1964 Inhomogeneous electron gas *Phys. Rev.* **136** B864
[45] John P, Ruzsinszky A, Csonka G I, Vydrov O A, Scuseria G E, Constantin L A, Zhou A and Burke K 2008 Restoring the density-gradient expansion for exchange in solids and surfaces *Phys. Rev. Lett.* **100** 136406
[46] John P, Burke K and Ernzerhof M 1996 Generalized gradient approximation made simple *Phys. Rev. Lett.* **77** 3865
[47] Becke A D and Johnson E R 2006 A simple effective potential for exchange *J. Chem. Phys.* **124** 221101
[48] Blochl P E, Jepsen O and Andersen O K 1994 Improved tetrahedron method for Brillouin-zone integrations *Phys. Rev. B* **49** 16223
[49] Georg M K H and Singh D J 2006 BoltzTraP. a code for calculating band-structure dependent quantities *Comput. Phys. Commun.* **175** 67–71
[50] Ramay S M, Hassan M, Mahmood Q and Mahmood A 2017 The study of electronic, magnetic, magneto-optical, and thermoelectric properties of XCr_2O_4 (X = Zn, Cd) through modified Becke and Johnson potential scheme (mBJ) *Curr. Appl Phys.* **17** 1038–45
[51] Mahmood Q, Hassan M, Ahmad S H A, Bhamu K C, Mahmood A and Ramay S M 2019 Study of electronic, magnetic, and thermoelectric properties of AV_2O_4 (A = Zn, Cd, Hg) by using DFT approach *J. Phys. Chem. Solids* **128** 283–90
[52] Al-anazy M M *et al* 2021 First principle study of optoelectronic and thermoelectric properties of magnesium based MgX_2O_4 (X = Sb, Bi) spinels *J. Solid State Chemistry* **303** 122480

[53] Aravindan V, Rajarajan A K and Mahendran M 2021 First-principles study of structural, electronic, magnetic and elastic properties of the Mn_2XSb (X = Co, Fe) inverse heusler *Alloys J. Electronic Materials* **50** 1786–93
[54] Ali M A, Ullah R, Abdullah S, Khan M A, Murtaza G, Laref A and Kattan N A 2021 An investigation of half-metallic variant perovskites A_2NbCl_6 (A = K, Rb) for spintronic based applications *J. Solid State Chemistry* **293** 121823
[55] Blundell S 2003 *Magnetism in Condensed Matter* **71** 94–5
[56] Sasıoglu E L, Sandanski M and Bruno P 2004 First-principles calculation of the intersublattice exchange interactions and curie temperatures of the full Heusler alloys Ni_2 Mn X (X = Ga, in, Sn, Sb) *Phys. Rev. B* **70** 024427
[57] De Gennes P G 1960 Effects of double exchange in magnetic crystals *Phys. Rev.* **118** 141
[58] Zhang H, Liu W, Lin T, Wang W and Liu G 2019 Phase stability and magnetic properties of Mn_3Z (Z = Al, Ga, In, Tl, Ge, Sn, Pb) heusler alloys *Appl. Sci.* **9** 964
[59] Mahmood Q, Alshahrani T, Haq B U, Gulfam Q, Tahir Y, Kattan N A, Fatima M and Laref A 2020 Role of 5d orbital of Re in ferromagnetism and thermoelectric characteristics of Cs_2ReCl/Br_6 double perovskites: a density functional theory studies *The European Physical Journal Plus* **135** 1–13
[60] Mahmood Q, Noor N A, Jadan M, Addasi J S, Mahmood A and Ramay S M 2020 First-Principle investigation of ferromagnetism and thermoelectric characteristics of $MgCr_2X_4$ (X = S, Se) spinels J *Solid-State Chem* **285** 121261
[61] Anh L D, Hai P N and Tanaka M 2016 Observation of spontaneous spin-splitting in the band structure of an n-type zinc-blende ferromagnetic semiconductor *Nat. Commun.* **7** 1–8
[62] Kant C J D, Tsurkan V and Loidl A 2010 Magnetic susceptibility of the frustrated spinels $ZnCr_2O_4$, $MgCr_2O_4$ and $CdCr_2O_4$ *J. Phys: Conf. Ser* **200** 032032
[63] Dietl T, Ohno O H, Matsukura A F, Cibert J and Ferrand E D 2000 Zener model description of ferromagnetism in zinc-blende magnetic semiconductors *Science* **287** 1019–22